

Mechanism of Electron Emission from Al(100) Bombarded by Slow Li^+ Ions

J. A. Yarmoff, T. D. Liu, and S. R. Qiu

*Department of Physics, University of California, Riverside, California 92521
and Materials Sciences Division, Lawrence Berkeley National Laboratory, Berkeley, California 94720*

Z. Sroubek

*Institute of Radio Engineering and Electronics, Academy of Sciences of Czech Republic,
Chaberská 57, 182 51 Praha 8, Czech Republic*

(Received 19 September 1997)

Emission of electrons from Al(100) during bombardment by 50–520 eV Li^+ ions was measured as a function of incident ion energy and direction. The process was modeled by a surface electron-hole pair excitation mechanism and was quantified with a one-electron parametric theory. This is a previously unidentified mechanism which is characterized by a strong dependence on the energy and angle of incidence of the primary particle. Good agreement between the experimental data and theory is found, which indicates that this mechanism is indeed responsible for electron emission during Li-Ai collisions. [S0031-9007(98)05512-4]

PACS numbers: 79.20.Rf, 79.20.Ap, 79.60.Bm

Kinetic electron emission (KEE) during collisions of slow ions with surfaces is a phenomenon that is not yet fully understood. There are several processes responsible for electronic excitation that lead to electron emission, but only in a few experiments have microscopic mechanisms of excitation been resolved and identified.

Kinetic electron emission due to the time-dependent perturbation of semilocalized atomic electrons by the nearby passage of an incompletely screened charge has been found to be dominant in the interaction of light ions (H^+ , He^+) with *d*-electron metals (Cu) [1]. For more energetic collisions, deep-level electron promotion processes [2] and direct particle-electron binary collisions [3,4] become prevalent. For collisions involving slow heavy rare-gas ions, KEE is usually masked by the much stronger potential emission. In cases where potential emission can be excluded, the mechanism of experimentally observed emission is still a matter of controversy [5–7]. Autoionization [6] and many-electron processes [7] have been suggested as possible sources of KEE in the low energy regime. Finally, electron emission has been found to be strongly dependent upon the cleanliness of the sample. For example, adsorbed oxygen on the surface of Al dramatically increases the electron yield [8] and the experiments indicate that the often observed weak electron emission from seemingly clean surfaces could be due to unintentional impurities.

In this Letter, we experimentally measure KEE resulting from Li-Al collisions at low energies. The energies employed are below the threshold for excitation of deep levels in the solid or projectile [9]. This eliminates contributions from cascading electrons that originate from core excitations. We then provide a quantitative theoretical description of the process in terms of a surface electron-hole pair excitation mechanism. This is a previously unidentified KEE mechanism which is characterized by a strong

dependence on the energy and angle of incidence of the primary particle.

An essential prerequisite for such a process to be efficient is a close energy match between the valence orbital of the particle and the Fermi level of the substrate. For example, this mechanism is less relevant for rare-gas particles with high ionization energies. In the present paper, we used Li^+ ions and an Al(100) substrate. The ionization energy of Li is 5.39 eV, which is very close to the Al(100) work function value of 4.41 eV. Furthermore, the Li-Al system has been thoroughly studied by several surface techniques, including ion scattering [9,10]. The measured resonant neutralization probabilities from these scattering experiments were successfully interpreted in terms of a one-electron parametric theory [10,11] based on the Anderson Hamiltonian. We employ a similar theoretical approach here, using the same parameters as in Ref. [11], to describe our KEE experiments.

The experiments were performed in the ultrahigh vacuum chamber (base pressure = 1×10^{-10} torr) that was previously used in Refs. [9,10]. The sample was cleaned by Ar^+ sputtering followed by annealing, while the cleanliness was monitored by Auger electron spectroscopy collected with a Perkin-Elmer cylindrical mirror analyzer. No surface oxygen was detected (to an estimated limit of 0.1% of a monolayer), and the level of carbon contamination was below 0.5% of a monolayer. The sample crystallinity was checked with low energy electron diffraction. Isotopically pure $^7\text{Li}^+$ ions were produced by a Kimball Physics ion gun which is (now) mounted onto a rotatable turntable that allows for independent variation of the incident ion beam direction. The beam current was measured prior to the collection of each spectrum by a Faraday cup attached to the sample manipulator, and all of the data were normalized by these values. Scattered ions and emitted electrons were collected with

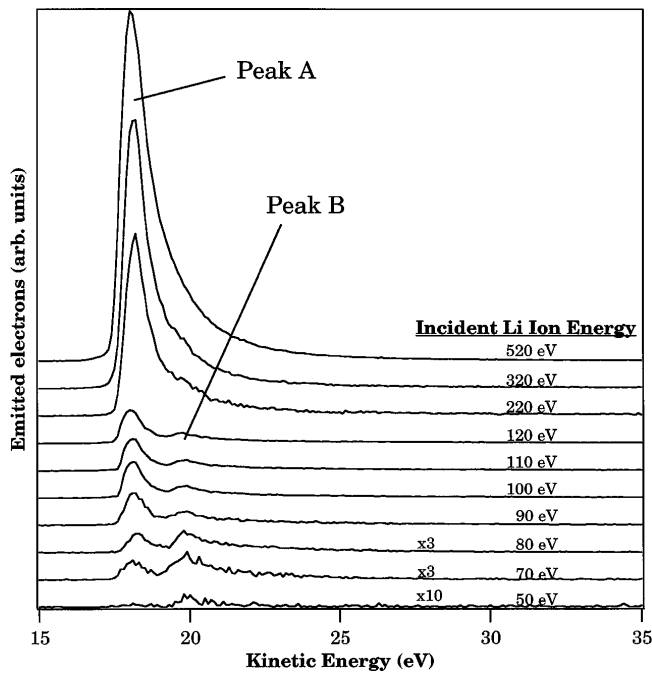


FIG. 1. Energy spectra of the electrons emitted from Al(100) under bombardment by ${}^7\text{Li}^+$ ions of the indicated energy. The ions were incident at $\theta = 13.4^\circ$ from the surface normal, while the electrons were collected at normal emission. There was a bias of -20 V placed on the sample.

a Comstock hemispherical energy analyzer that has an angular acceptance of $\pm 2^\circ$, and was operated in constant pass energy mode. A small negative bias voltage (-10 to -20 V) was applied to the sample in order to accelerate the zero-kinetic energy electrons to the analyzer. Note that this bias voltage also acted to increase the primary beam energy (the energies reported here include this effect). For the data presented in this paper, electrons were always collected at normal emission.

Figure 1 shows emitted electron energy spectra collected for various incident ${}^7\text{Li}^+$ beam energies. Although the data were collected with a -20 V bias on the sample, the cutoff appears at ~ 18 eV. This is because there is a difference between the sample and analyzer work functions of ~ 2 eV. The difference is due partly to the embedding of Li during the measurements, which slightly lowers the work function of the sample. Care was taken to insure that these work function changes were kept to a minimum, and therefore did not influence the shape of the spectra.

Spectra collected at normal emission using 210 eV ${}^7\text{Li}^+$ impinging at various incident angles are shown in Fig. 2. The spectra are labeled by the angle θ , which is the angle between the incident beam direction and the sample normal. Note that the yield of electrons is a rapidly decaying function of the incident angle, which explains why they may not have been observed in a previous investigation that employed a 60° incidence angle [8].

The spectra show one peak, labeled A, located just above the cutoff, while there is another, labeled B, located approximately 2 eV higher in energy. Peak A indicates the process that is the subject of this paper, and dominates at high incident ion energy and near-normal incidence. Potential emission cannot be responsible for this peak because the ionization energy of Li is too small so that the Auger electrons could not be emitted into the vacuum. The large intensity of peak A also excludes any emission process related to the presence of oxygen, since the amount of adsorbed oxygen is so small. Furthermore, we measured the intensity of Peak A as a function of oxygen coverage, and were able to demonstrate conclusively that it is not related to adsorbed oxygen. Peak B is also not due to adsorbed oxygen, but could be related to conventional sputtering of Al^- ions or to another mechanism of electron emission. New experimental data and possible mechanisms of the process responsible for Peak B will be presented elsewhere [12].

In order to quantify the results, the data were numerically integrated to obtain the area of peak A under various scattering conditions. Care was taken to include only the contribution from peak A, and to exclude any from peak B. Since the important parameter in the theoretical description of the process is the perpendicular component of the incident velocity, the integrated areas are plotted in Fig. 3 as a function of $1/(E^{1/2} \cos \theta)$, where E is the incident beam energy in eV. Because of the strong energy and angular dependencies of these yields, the areas are

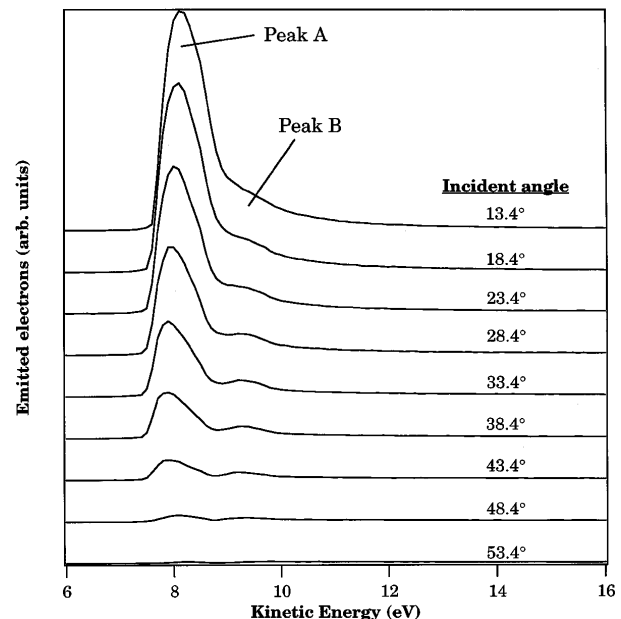


FIG. 2. Energy spectra of the electrons emitted from Al(100) under bombardment by 210 eV ${}^7\text{Li}^+$ ions. The ions were incident at the indicated angle θ with respect to the surface normal, while the electrons were collected at normal emission. There was a bias of -10 V placed on the sample.

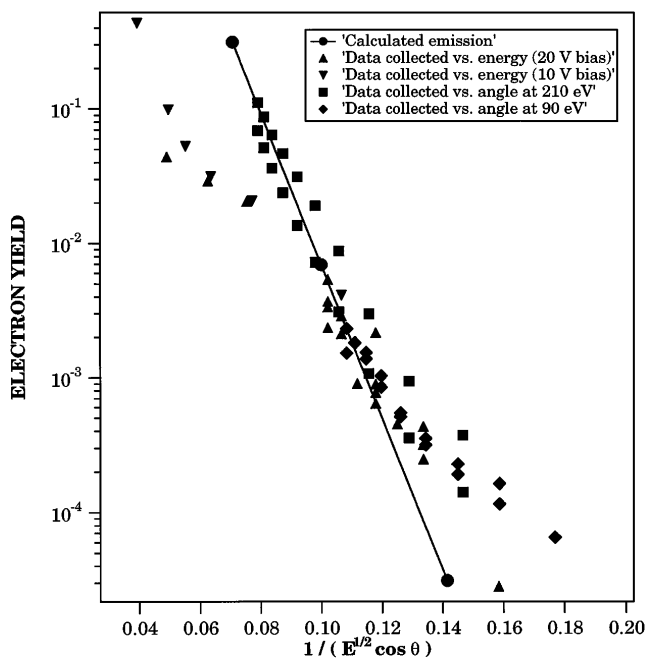


FIG. 3. Comparison of the calculated electron yield (●) to the experimental data. The x axis is proportional to the inverse value of the perpendicular velocity of the impinging Li^+ ion, i.e., to the inverse of the product of the square root of the Li^+ incident kinetic energy E (in eV) and the cosine of the incident angle θ . The integrated areas for peak A are shown for ions incident at $\theta = 13.4^\circ$ as the incident ion energy E is changed using a -20 V bias (▲) and a -10 V bias (▼). Also shown are integrated areas collected as the incident angle θ is changed using $E = 210$ eV (■) and $E = 90$ eV (◆). The calculated yields are shown on an absolute scale, while the experimental data have been arbitrarily normalized to the calculation.

plotted on a log scale. Shown in the figure are not only the integrated areas from the data in Figs. 1 and 2, but additional data as well. Each individual run is shown with a different symbol, and the data collected can be quantitatively compared within a single run. Since the absolute collection efficiency of the analyzer is unknown, data from the different runs have been arbitrarily aligned to each other and to the theoretical curve. Note, however, that the important result is the correspondence between the slopes of the various curves.

$$n(\varepsilon_k) = \frac{1}{\pi^2} \int_{-\infty}^{\varepsilon_f} d\varepsilon_{k'} \left| \int_{-\infty}^{\infty} dt \frac{\Delta(t)}{i\Delta(t) + \varepsilon_{k'} - \varepsilon_a(t)} \exp[i(\varepsilon_k - \varepsilon_{k'})t] \right|^2. \quad (4)$$

The time dependence of $\varepsilon_a(t)$ and $\Delta(t)$ are obtained from (2) and (3) and from the dependence of z on time t . The trajectory $z(t)$ has been calculated for normal incidence using the Molière atomic interaction potential. Only the incoming part of the trajectory was used for determining the excitation.

The calculated values of $n(\varepsilon_k)$ were integrated from the vacuum level ε_v to about 2 eV above ε_v in order to include all experimentally detectable electrons. These

integrated values are shown in Fig. 3 by the solid circles. It is clear from Fig. 3 that the theoretical dependence of the excitation, and thus also of the emission, is close to $\exp(-A/v_\perp)$, where v_\perp is the perpendicular velocity of the impinging particle and A is a constant. This is a specific feature of the suggested emission mechanism.

$$H(t) = \varepsilon_a(t)c_a^\dagger c_a + \sum_k \varepsilon_k c_k^\dagger c_k + \sum_k (V_{ak}(t)c_a^\dagger c_k + \text{c.c.}), \quad (1)$$

where $\varepsilon_a(t)$ is the Li $2s$ ionization energy which depends upon the distance z (which depends upon the time t) of Li from the surface as [11]

$$\varepsilon_a(z) = \varepsilon_a(\infty) + \left[\frac{16z^2}{e^4} + \frac{1}{E_c^2} \right]^{-1/2}. \quad (2)$$

$\varepsilon_a(\infty) = -5.4$ eV is the ionization energy of Li and $E_c = 2.6$ eV is the cutoff in the image potential [11]. ε_k are the energies of the metal orbitals and $V_{ak}(t)$ are the transfer matrix elements between orbitals a and k . V_{ak} depends upon the distance z as [11]

$$V(z) = V \exp \left[\frac{-3.88}{z} - 0.4916z \right] \quad (\text{distances in a.u.}). \quad (3)$$

The value of V is adjusted to give the appropriate value [11] of the virtual half-width Δ of the Li $2s$ level (for the distance $z = 4$, the value of Δ is 1.34 eV) and $\Delta(z)$ depends upon $V(z)$ quadratically.

The solution of the Hamiltonian (1) for electron excitation, i.e., for electron-hole pair excitation in the metal, can be found either by numerically solving the set of differential equations for operators c_a and c_k if the k levels are discrete or the solution can be put in a more compact integral form when the slowness approximation and a continuum of k levels are used [13,14]. In the latter case, the expression (using $\hbar = 1$) for the number of electrons excited between ε_k and $\varepsilon_k + d\varepsilon_k$ is given by the integral

integrated values are shown in Fig. 3 by the solid circles. It is clear from Fig. 3 that the theoretical dependence of the excitation, and thus also of the emission, is close to $\exp(-A/v_\perp)$, where v_\perp is the perpendicular velocity of the impinging particle and A is a constant. This is a specific feature of the suggested emission mechanism.

The experimentally observed dependence of the electron emission on the primary ion energy E and on the angle θ agree closely with those theoretically predicted.

This is strong evidence that the surface electron-hole pair excitation mechanism is indeed responsible for the observed electron emission. Another mechanism of electron excitation and emission which derives from (1) is the autoionization of the Li $2s$ level when the level moves above the vacuum level. But the large broadening of this level at small distances z renders the autoionization process very improbable in this case [14].

Although the experimental data and the theoretical description are in large part in agreement, there are some deviations. At high energies, i.e., to the left of Fig. 3, the theory overestimates the electron yield. This overestimate may have contributions from two sources. First, as the energy is raised there is an increased probability that Li projectiles would embed in the lattice, rather than simply scatter. Those projectiles would have a decreased probability for KEE excitation, and the yield would therefore be reduced from that predicted. Second, the angular distributions of the emitted electrons should change as the energy is raised above the vacuum level. For zero-kinetic energy electrons, the angular distributions will be sharply peaked towards the normal as the only force acting upon them is the field due to the applied bias voltage. As the energy of the electrons increases, however, the angular distribution should become more dispersed. As seen in Fig. 1, peak A broadens with increasing incident energy, so that the contribution of off-normal electrons should also increase. Since our analyzer collected only those electrons emitted within 2° of the normal, the measured yield likely underestimates the total emitted yield as the incidence energy increases.

Both of these sources for deviation between experiment and calculation are not, however, expected to contribute to the data collected as a function of θ at constant E , such as shown in Fig. 2 and by the solid square and solid diamond symbols in Fig. 3. In this case, the probability for Li embedding into the lattice is not strongly angle dependent, and also the width of peak A does not change with θ . So, it is expected that the experimental angular data would have the greatest correspondence with the theory, which is exactly what is seen in Fig. 3.

Note that there is also a small deviation between experiment and theory at low energies and high angles, i.e., on the right of Fig. 3, in which the theory underestimates

the number of emitted electrons. This is possibly due to a contribution from yet another process that dominates when the proposed mechanism cannot occur. One such process could be, for example, the collisional mechanism discussed in Ref. [7] which is characterized by a smaller intensity and by a much smaller dependence on the projectile energy than the mechanism discussed in this paper.

A surface electron-hole pair excitation process due to impact of slow Li particles on the clean Al(100) surface has been identified as a source of secondary electrons. The identification is based on a comparison of experimental results with the parametrical one-electron theory that was used previously in a successful interpretation of Li-Al data [10]. The theory predicts a sharp dependence of the electron emission on the angle of incidence and on the energy of the primary particles, in close agreement with experiment.

The authors wish to acknowledge the National Science Foundation Award No. INT-9600473 and the Czech Academic Grant No. 67501 for financial support.

-
- [1] G. Spierings, I. Urazgil'din, P. A. Ziejlman van Emmichoven, and A. Niehaus, *Phys. Rev. Lett.* **74**, 4543 (1995).
 - [2] N. Fano and W. Lichten, *Phys. Rev. Lett.* **14**, 627 (1965).
 - [3] B. A. Trubnikov and Y. N. Yavlinskii, *Sov. Phys. JETP* **21**, 167 (1965).
 - [4] R. A. Baragiola, E. V. Alonso, J. Ferrón, and A. Oliva-Florio, *Surf. Sci.* **90**, 240 (1979).
 - [5] E. V. Alonso, M. A. Alurralde, and R. A. Baragiola, *Surf. Sci.* **166**, L155 (1986).
 - [6] G. Lakits, F. Aumayr, M. Heim, and H. P. Winter, *Phys. Rev. A* **42**, 5780 (1990).
 - [7] Z. Sroubek, *Phys. Rev. Lett.* **78**, 3204 (1997).
 - [8] J. C. Tucek and R. L. Champion, *Surf. Sci.* **382**, 137 (1997).
 - [9] K. A. H. German, C. B. Weare, and J. A. Yarmoff, *Phys. Rev. B* **50**, 14452 (1994).
 - [10] C. B. Weare and J. A. Yarmoff, *Surf. Sci.* **348**, 359 (1996).
 - [11] J. B. Marston, D. R. Andersson, E. R. Behringer, and B. H. Cooper, *Phys. Rev. B* **48**, 7809 (1993).
 - [12] J. A. Yarmoff and Z. Sroubek (unpublished).
 - [13] R. Brako and D. M. Newns, *J. Phys. C* **14**, 3065 (1981).
 - [14] Z. Sroubek and J. Fine, *Phys. Rev. B* **51**, 5635 (1995).